

# Application of Hybrid Optimization Technique for Tuning PID Controller in LabVIEW-Multisim Integrated Cuk converter

T.Mariammal, T.Deepa  
SELECT, VIT University, Chennai.

**Abstract:** A novel design for optimizing the parameters of the Proportional, Integral (PI) controller using Particle Swarm Optimization-Gravitational Search Algorithm (PSO-GSA) was proposed. First, Cuk converter was designed in the continuous conduction mode. Then a PI controller was designed with the objective of set point tracking of output voltage of the converter and to minimize the performance index such as Integral Absolute Error (IAE)). The parameters of PI controller were optimized to control the output voltage of the converter. The optimization was carried in an Intel i5 core processor for 50 trials with 100 iterations for each trial. It was found that the proposed PSOGSA optimization provides faster convergence and a better solution in terms of integral absolute error.

**Key words:** DC-DC converter, Set point tracking, Optimization, PID controller, PSO, PSOGSA.

## 1. Introduction

Over the past few decades, despite all advances in process control, Proportional-Integral-Derivative (PID) controller is still the common controller in many applications. The main reason for that is the robustness, simplicity and easy implementation options provided by PID based control structures. The flexibility of the controller makes it suitable for use in many control applications. The design strategies of PID controller mainly aim at minimizing errors like Integral Absolute Error (IAE), Integral Square Error (ISE), and Integral Time Absolute Error (ITAE) and thereby improving the performance indices of the controller. Some of the common artificial Intelligence techniques such as neural networks, fuzzy logic and genetic algorithms had been widely employed to fine tune the PID parameters. Recently bio-inspired algorithms such as Particle Swarm Optimization (PSO), Bacteria Foraging Optimization Algorithm (BFOA), Firefly Fly Optimization Algorithm, Artificial Bee Colony (ABC) were gaining importance and play a major role in optimizing the parameters of PID controllers. This paper mainly focuses on PSOGSA algorithm for optimal tuning of PI controller.

DC-DC converters are gaining importance nowadays in power processing systems rather than signal processing systems. In Power electronic systems, the DC-DC converters play a vital role in controlling the power from the source to the load with maximum efficiency. The functions of power processing systems include voltage regulation, maximum power transfer and its association with other processes [1]. Though the converters are capable of transferring the voltage from lower to higher or vice versa, their energy transport mechanism forms the foundation for the building block of such converters. The various converter topologies are buck, boost and buck-boost and some of the derived topologies such as Cuk[9], SEPIC[8] are also widely employed in varied applications. Among these topologies, Cuk converter was chosen since it has continuous input current,

continuous output current and the output voltage can be lesser or greater than the input voltage [4].Deivasundari et al presented a reduced order model of a zero average dynamics controlled DC-DC Cuk converter which was designed based on moment matching techniques [5].

Cuk converter implementing PI and PI-SMC control were compared and presented [6]. SEPIC converter employing a Fuzzy logic controller was proposed for a photovoltaic system [7].Hossein Komijani et al modeled and designed a state feedback controller for a tubular linear permanent magnet synchronous motor. The controller decreases the distortion of the waveform [8]. Thakur proposed a control technique for Cuk converter which works in highly perturbed system conditions such as input voltage and load variations [9]. Grey relational analysis combined with Taguchi method to optimize PID controller parameter for a multiobjective problem was explained in [10]. A study to understand the robustness of PID controller tuning methods to step changes in set point and disturbance rejection in power converter control was discussed in [11].

K. Trojanowski and T. Kulpa [12] presented a new evaluation of particle convergence time based on theoretical analysis of properties of the particle in the model with respect to inertia weight. A method for designing the optimal PID controller parameters of a Permanent magnet DC motor using PSO showing the advantages of easy implementation, fast convergence and good computational efficiency over Z-N method was discussed [13]. In [14], PID was optimally tuned using PSO-BFO algorithm in which initial searches are carried out in parallel using BFO and the search results are fine tuned using PSO. The parameters of a fractional order PID controller was optimized using PSO and the performance for the same is studied in a PV system [15]. T. Deepa and P. Lakshmi presented a comparison of GSA and PSO in tuning a PI controller for a multivariable four tank system and found that PSO was superior in regulation [16].

This paper is organized as follows. Section II explains the circuit model of Cuk converter. Section III explains the PID controller. Section IV describes the tuning algorithms and its implementation. Section V discusses the results and conclusion.

## 2. Model of Cuk Converter

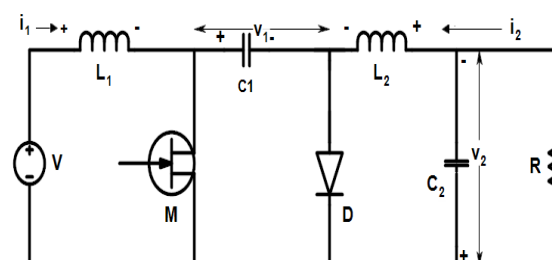


Fig.1a Cuk converter model

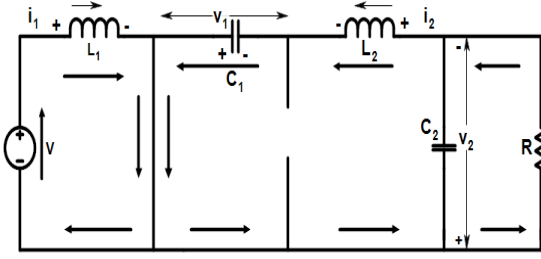


Fig.1b Cuk converter ON state

Fig.1a shows the model of a Cuk converter. The converter is a step-down/step-up converter based on a switching buck-boost topology. It works by capacitive energy transfer. The converter contains two stages. One is the input stage and the other an output stage. The input voltage is fed into the circuit through the inductor  $L_1$ . Fig 1b shows the ON state mode of Cuk converter. When the switch is ON, the current  $i_1$  builds up magnetic energy in the input inductor. The diode is reverse biased and the energy is dissipated from the capacitor in the output stage.

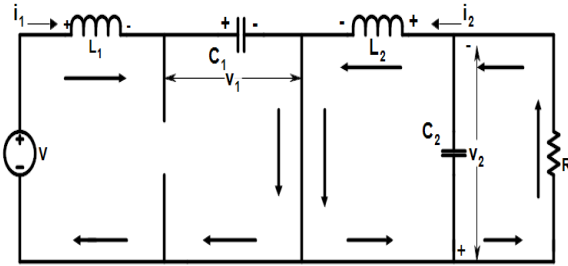


Fig.1c Cuk converter OFF state

Fig 1c shows the Cuk converter in OFF state. When the switch is turned OFF, the inductor tries to maintain the current in the same direction by reversing its polarity. It thus provides energy to the output stage through the capacitor  $C_1$ .

## 2.1 Cuk converter design

### Design equations

Input Voltage  $V = 100V$

Frequency  $f = 100 \text{ KHz}$

Duty cycle  $D = 0.5$

Resistance  $R = 10 \text{ ohms}$

$$i_1 = \frac{VD^2}{R(1-D)^2} = 10 \text{ A} \quad (1)$$

$$i_1 = \frac{VD^2}{R(1-D)^2} = 10 \text{ A} \quad (2)$$

$$v_1 = \frac{V}{(1-D)} = 200 \text{ V} \quad (3)$$

$$v_2 = \frac{-VD}{1-D} = -100 \text{ V} \quad (4)$$

Assuming the output ripple voltage is 5% of the output voltage

$$\Delta v_2 = \frac{(v_1 + v_2)D}{8f^2 L_2 C_2} = 5V \quad (5)$$

$$\Rightarrow L_2 C_2 \geq 8.25 \times 10^{-6}$$

Assuming  $L_2 = 30\text{mH}$ ,  $C_2 = 50\mu\text{F}$ , The converter is required to operate in continuous conduction mode. This

requires that only positive currents flow through the diode.

$$\frac{\Delta i_1 + \Delta i_2}{2} < I_1 + I_2$$

$$\Delta i_1 = \frac{VD}{L_1 f} = 0.022 \text{ A} \quad (6)$$

$$\Delta i_2 = \frac{VD}{L_2 f} = 0.022 \text{ A} \quad (7)$$

$$L_1 = \frac{L_2 RT (1-D)^2}{2L_2 - RT(1-D)^2} = 30 \text{ mH} \quad (8)$$

$$C_1 > \frac{D^2 T}{2R} = 150 \mu\text{F}$$

The design parameters are listed in Table 1

TABLE 1 Design Parameters

Inductor $L_1$	30 mH
Inductor $L_2$	30 mH
Capacitor $C_1$	150 $\mu\text{F}$
Capacitor $C_2$	50 $\mu\text{F}$
Resistive load	10 $\Omega$
Input Voltage $V$	100 V
Reference Voltages $V_r$	-200 , - 50, -200 V

## 2.2 State space equations

The output to input transfer function can be obtained by applying state space analysis to the circuit.

### During ON time

$$\frac{di_1}{dt} = \frac{V}{L_1} \quad (9)$$

$$\frac{di_2}{dt} = \frac{v_1}{L_2} - \frac{v_2}{L_2} \quad (10)$$

$$\frac{dv_1}{dt} = -\frac{i_2}{C_1} \quad (11)$$

$$\frac{dv_2}{dt} = \frac{i_2}{C_2} - \frac{i_2}{RC_2} \quad (12)$$

### During OFF time

$$\frac{di_1}{dt} = \frac{V}{L_1} - \frac{v_1}{L_1} \quad (13)$$

$$\frac{di_2}{dt} = -\frac{v_2}{L_2} \quad (14)$$

$$\frac{dv_1}{dt} = \frac{i_1}{C_1} \quad (15)$$

$$\frac{dv_2}{dt} = \frac{i_2}{C_2} - \frac{v_2}{RC_2} \quad (16)$$

Where  $i_1$  is the current through the inductor  $L_1$ ,  
 $i_2$  is the current through the inductor  $L_2$ ,  
 $v_1$  is the voltage across the capacitor  $C_1$ ,  
 $v_2$  is the voltage across the capacitor  $C_2$ ,  
 $V$  is the input voltage.

$u$  is the control signal.  $u=0$  when the switch is in the OFF state and  $u=1$  when the switch is in the ON state.

With the circuit defined over the two intervals, the A, B, C, E matrices can be defined as shown below:

$$A_1 = \begin{bmatrix} 0 & 0 & 0 & 0 \\ 0 & 0 & \frac{1}{L_2} & -\frac{1}{L_2} \\ 0 & \frac{-1}{C_1} & 0 & 0 \\ 0 & \frac{1}{C_2} & 0 & -\frac{1}{RC_2} \end{bmatrix}$$

$$A_2 = \begin{bmatrix} 0 & 0 & \frac{-1}{L_1} & 0 \\ 0 & 0 & 0 & \frac{-1}{L_2} \\ \frac{1}{C_1} & 0 & 0 & 0 \\ 0 & \frac{1}{C_2} & 0 & \frac{-1}{RC_2} \end{bmatrix}$$

$$B_1 = B_2 = B = \begin{bmatrix} \frac{1}{L_1} \\ 0 \\ 0 \\ 0 \end{bmatrix}$$

$$C_1 = C_2 = C = [0 \quad 0 \quad 0 \quad 1]$$

$$E_1 = E_2 = E = [0 \quad 0 \quad 0 \quad 0]$$

$$A = A_1 D + A_2 D' \quad (17)$$

$$B = B_1 D + B_2 D' \quad (18)$$

$$C = C_1 D + C_2 D' \quad (19)$$

$$E = E_1 D + E_2 D' \quad (20)$$

Where  $D'=1-D$

A state space averaged model that describes the converter in equilibrium is

$$\dot{x} = AX + BU \quad (21)$$

$$Y = CX + EU \quad (22)$$

The above equation (21) & (22) can be used to obtain the equilibrium state and the output vector.

To simplify the model, it is linearized by considering small perturbations in the variables. A graph is plotted between the duty cycle and the output voltage.

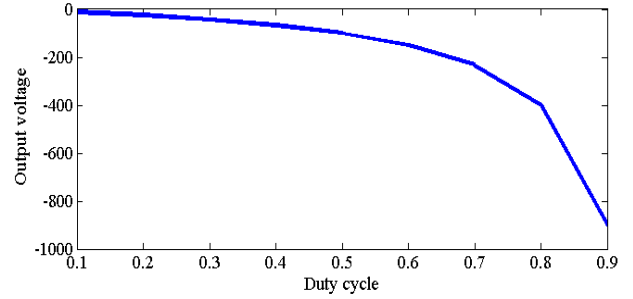


Fig.2 Output voltage Vs duty cycle

From 0.8 to 0.9 duty cycle, the graph shows a linear region. Around the operating point, the converter exhibits linear characteristics. Hence a duty cycle of 0.8 is chosen. Proper PI gains guarantee that the equilibrium point is linear. Hence a PI controller is added with the converter.

### 2.3 Transfer Function

With the state spaces defined, the transfer function can be calculated using

$$\frac{V_0}{V} = C(SI - A)^{-1} B \quad (23)$$

$$\text{The transfer function is } G(S) = \quad (24)$$

$$G(S) = \frac{2.37e^{10}}{S^4 + 200S^3 + 8.178e^5 S^2 + 3.022e^7 S + 5.92e^9}$$

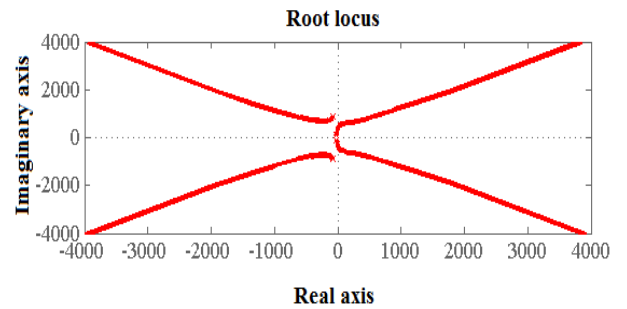


Fig. 3.1 Root locus diagram showing the location of poles

Poles are

$$\begin{aligned} &1.0e+02 * \\ &-0.8197 + 8.9320i \\ &-0.8197 - 8.9320i \\ &-0.1803 + 0.8391i \\ &-0.1803 - 0.8391i. \end{aligned}$$

Fig 3.1 shows the root locus graph showing the location of poles in the S-plane. From the graph, it was observed that the poles are located in the left half of S-plane. So the system is stable.

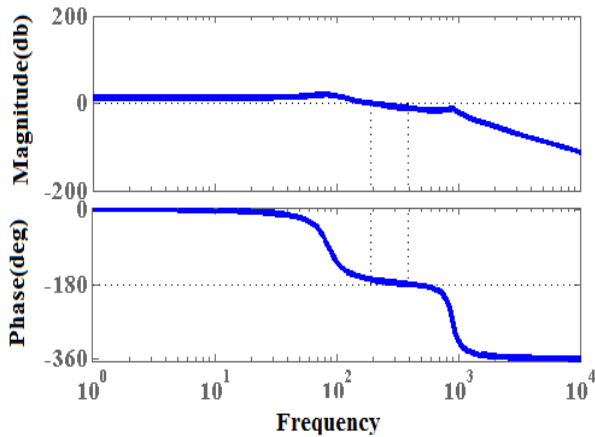


Fig.3.2 Bode diagram

Gain Margin = 12 db.

Phase Margin = 10.7 deg.

The Power stage circuit of the Cuk converter simulated using Multisim with the Co-simulation terminals was shown in Fig.3.3.

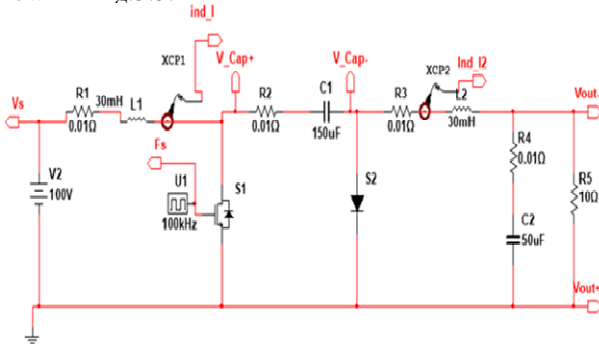


Fig.3.3 Cuk Converter simulation circuit in Multisim

The LABVIEW Control and Design simulation loop connected to Multisim with Multisim design Interface block is shown in Fig 4. The converter was designed for an input voltage of 100V and the MOSFET switch was pulsed with the frequency of 100 KHz. The duty ratio can be varied from 0 to 1. The control knob was adjusted for varying the duty cycle and the dynamic behaviour of the circuit for 0.5 variation in duty ratio was studied. Fig 5 shows the inductor currents  $i_1, i_2$  and the Capacitor voltages  $v_1$  and  $v_2$  at 100KHz frequency for a duty ratio of 0.5.

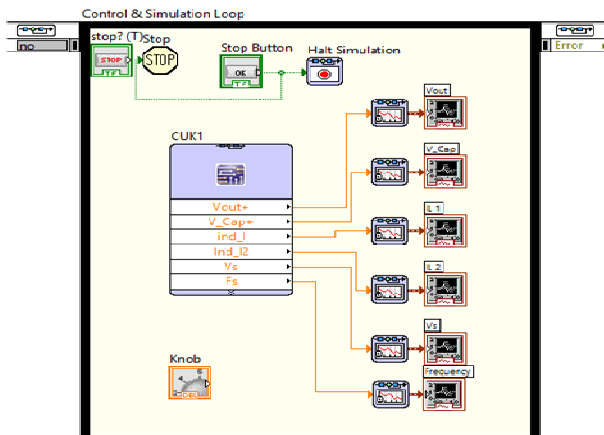


Fig.4 Cuk converter simulation circuit integrated with LabVIEW

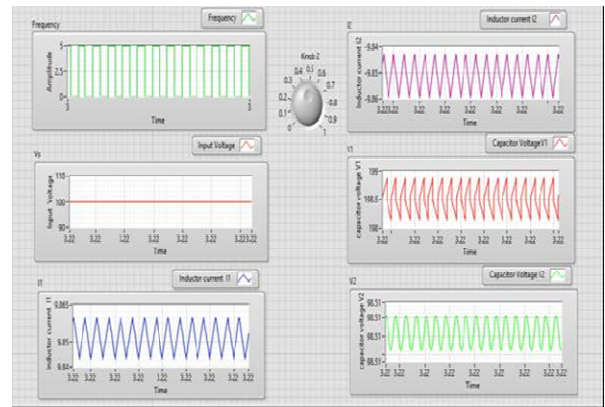
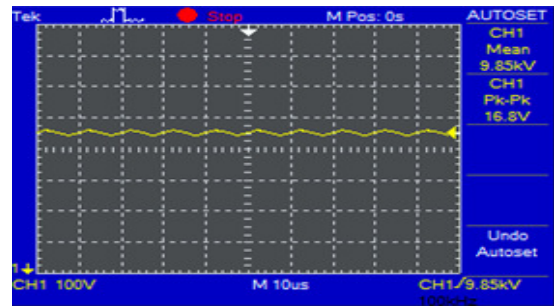


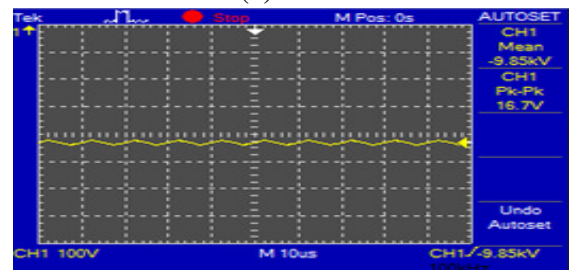
Fig.5 Inductor currents and Capacitor voltages in LabVIEW

## 2.4 Hardware in-loop

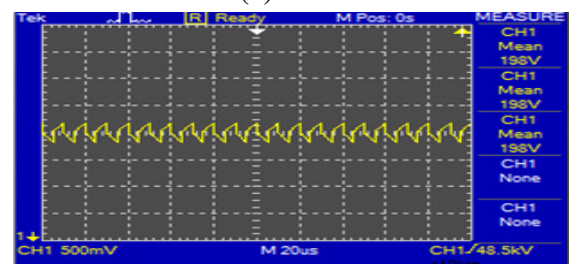
Cuk converter was constructed in Hardware-in-loop (HIL). The converter was fed with an input voltage of 100 V. Fig 6.a shows the Inductor currents  $i_1$  and  $i_2$  obtained from channel 1 of digital storage oscilloscope. The Inductor 1 shows a current of 9.85A and the inductor 2 shows a current of -9.85 A. Fig 6.b shows the Capacitor voltages  $v_1$  and  $v_2$ . They were observed as 198V and -98.5V respectively. The switching frequency was set at 100 KHz.



6(a)

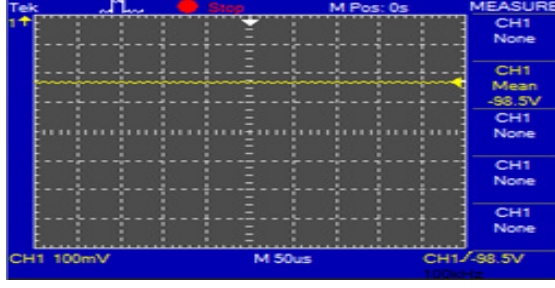


6(a)



6(b)





6(b)  
Fig 6.a.Waveforms of Inductor current  $i_{L1}, i_{L2}$ , and  
6.b. capacitor voltages  $v_{C1}, v_{C2}$ .

### 3. PID Controller

PID controller is one of the earliest control strategies. It has a simple control structure and hence easy to implement. PID controller has three terms. Proportional term produces an output proportional to the error signal, Integral term produces an output proportional to the integral of error signal and derivative controller produces an output proportional to the derivative of error signal. Proportional controller increases the overshoot, integral controller reduces the steady state error and the derivative controller dampens the response. Here PI controller is used, as the derivative term is sensitive to noise and during steady state, the system is very steady due to the absence of derivative term. The general structure of PID controller is

$$u(t) = K_p \left[ e(t) + \frac{1}{T_i} \int e(t) dt + T_d \frac{de(t)}{dt} \right] \quad (25)$$

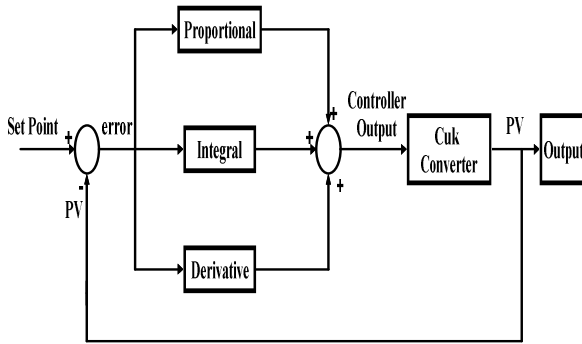


Fig.7 Block diagram of Set point tracking of Output Voltage of Cuk converter

#### 3.1 Set Point tracking

Set point tracking is used to track the output voltage. The structure of PI controller is given by

$$G_c(S) = K_p + \frac{K_i}{S} \quad (26)$$

Where  $G_c(S)$  is the transfer function of the PI controller.  $K_p$  is the proportional gain and  $K_i$  is the integral gain.

#### 3.2 Tuning of PI Controller

The controller parameters were obtained by Zeigler-Nichols method of tuning. In this method, the proportional gain was varied keeping Integral value as zero till sustained oscillations were obtained. Based on the critical time period ( $T_{cr}$ ) and critical gain ( $K_{cr}$ ), the values of proportional gain and integral gains were calculated. The

critical gain and critical time period was 3.858 and 0.044344. Hence the values of  $K_p$  and  $K_i$  obtained by Zeigler-Nichol's method was  $K_p=1.929$  and  $K_i=0.02272$ .

The closed loop transfer function of a plant and controller with negative unity feedback system is given by

$$P(S) = \frac{G(S)G_c(S)}{1 + G(S)G_c(S)} \quad (27)$$

The closed loop transfer function with the values of  $K_p$  and  $K_i$  obtained from Zeigler-Nichol's method is  $P(S) =$

$$\frac{4.57173e10 + 5.25476e8}{S^5 + 200S^4 + 3.022e^7 S + 5.16433e^{10} S + 5.25476e^8} \quad (28)$$

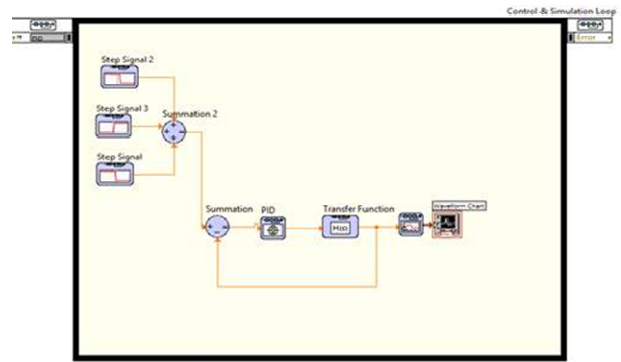


Fig.8 Simulation of Cuk converter with PID controller in Lab VIEW

Fig. 8 shows the simulation of Cuk converter with PID controller. Fig. 8 shows the response waveform for  $V_r = -200V$  from 0 to 0.5sec,  $V_r = -50V$  from 0.5 to 1.0 sec and  $V_r = -200V$  from 1.0 to 1.5 sec. The converter tracks the output voltage maintaining good voltage regulation.

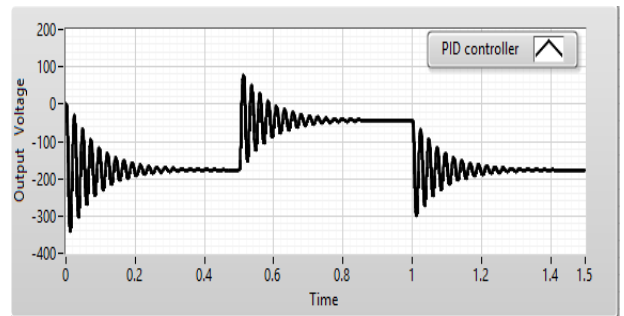


Fig.9 Output voltage waveform of PID controller with Cuk converter

### 4. Particle Swarm Optimization

PSO is a robust stochastic optimization technique based on the movement and intelligence of swarms. It was developed in 1995 by James Kennedy and Russell Eberhart. PSO uses the concept of social interaction to problem solving. Each particle is searching for an optimum and is moving with the velocity. Each particle remembers the position where it has its best result so far. This value is called personal best pbest. They co-operate and exchange the information that they have discovered in the places they visited. The information got from other particle is gbest. The great advantage of PSO is its computational efficiency.

#### 4.1 Implementation of PSO algorithm

Each particle has two state variables. They are: its current position and its current velocity. Each particle has a small memory in which each has its personal best position and the global best position experienced so far. One is considered better than the other and it gives lower value for the objective function. For each particle, the position vector and the velocity vector are selected at random from a predetermined search range. After the particles are initialized, the iterative optimization process starts, where the position and the velocities of the particles are updated by the equations.

$$V_{id} = w \times V_{id} + C_1 r_1 \times (P_{id} - X_{id}) + C_2 r_2 \times (G_{id} - X_{id}) \quad (29)$$

$$X_{id} = X_{id} + V_{id} \quad (30)$$

Where  $i$  is the no of particles,  $d$  is the dimension,  $C_1$  and  $C_2$  are acceleration Co-efficients,  $w$  is the inertia weight and  $r_1$  and  $r_2$  are uniformly random numbers. The algorithm is ended when the stopping criterion is met. Two commonly used Performance indices, namely Integral Absolute Error (IAE) and Integral Time Absolute Error were obtained. A subprogram is written as an objective function for the minimization of absolute error and this is called by the main program. The aim of the algorithm is to find the controller parameters that minimize the IAE criteria. Mathematically it can be represented as

$$IAE = \int abs(r(t) - y(t)) dt \quad (31)$$

where  $r(t)$  is the reference signal and  $y(t)$  is the output signal. The parameters of PSO algorithm are listed in table 2 and Fig.9 shows the flow chart of PSO algorithm.

**Table 2 PSO Parameters**

Maximum Iteration	100
Population	100
Inertia Weight $w$	1
Acceleration Co-efficient $C_1$	1.5
Acceleration Co-efficient $C_2$	2
Lower bounds $K_p$	0.01
Lower bounds $K_i$	200
No. of variables	50

#### 4.2 Flow Chart

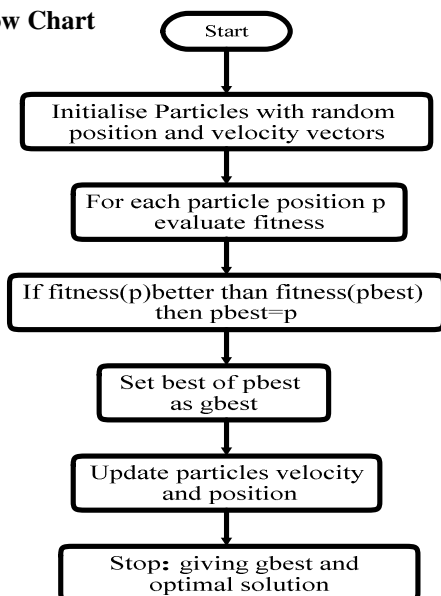


Fig.9 Flowchart of PSO algorithm

The closed loop transfer function of the plant and controller with unity negative feedback with the optimized values of  $K_p$  and  $K_i$  is  $C(S)/R(S) =$

$$\frac{2.18016e^{10}S + 4.7459e^{10}}{S^5 + 200S^4 + 817800S^3 + 3.022e^7S^2 + 2.77276e^{10}S + 4.7459e^{10}} \quad (32)$$

The poles are

1.0e+02 \*  
 -0.8447 + 8.7735i  
 -0.8447 - 8.7735i  
 -0.1467 + 1.8818i  
 -0.1467 - 1.8818i  
 -0.0171 + 0.0000i

All the poles are located in the left half of S-plane, denoting a stable system. The response curve of a stable higher order system is the sum of exponential curves and damped sinusoidal curves. Since the system is stable, the exponential terms and damped exponential terms will approach zero as time  $t$  increases. The type of transient response is determined by the closed loop poles while the shape of transient response is determined from the closed loop zeros. Whether a linear system is stable or unstable is a property of the system itself and does not depend on the input or driving function of the system. The poles of the input do not affect the stability of the system but contribute to the steady state response terms of the solution. The dominant pole is -1.71 which decides the transient behaviour of the system and the poles located farther from the imaginary axis than the original system corresponds to a more stable system. The voltage waveform for various values of reference voltage is obtained. Fig.10 shows the simulation of Cuk converter with PID and PSO-PID controller. Fig. 11a shows the response waveform for  $V_r = -200V$  from 0 to 0.5sec,  $V_r = -50V$  from 0.5 to 1.0 sec and  $V_r = -200V$  from 1.0 to 1.5 sec.

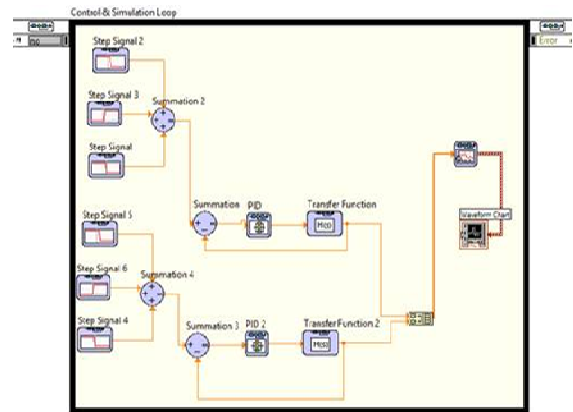


Fig 10 Simulation of PID and PSO-PID controller with Cuk converter in LabVIEW

#### 4.3 Simulation Results

Table.3 PSO optimized Proportional gain and Integral gain values

Controller	$K_p$	$K_i$	Best	Worst	Elapsed time
PSO-PID	0.9199	2.0025	52.0298	54.5584	564.5516

The optimization was run in i5 core processor with 50 trials. During each trial with 100 iterations the values of  $K_p$  and  $K_i$  were obtained. Minimization of error is the objective function and for that, the minimum and maximum values were tabulated as best and worst values respectively. The corresponding value of  $K_p$  and  $K_i$  were chosen and the best fitness curve was obtained for the same. The worst value was also tabulated in Table 3. Fig.11a shows the output voltage waveforms of the Cuk converter with PI and PSO-PI controller and Fig.11b shows the best fitness curve obtained for 100 iterations.

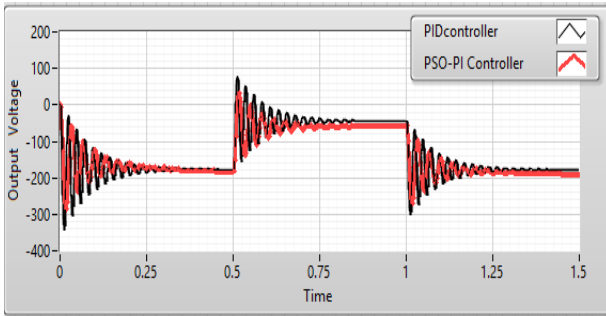


Fig.11a Output voltage waveforms of Cuk converter with PID and PSO-PI controller

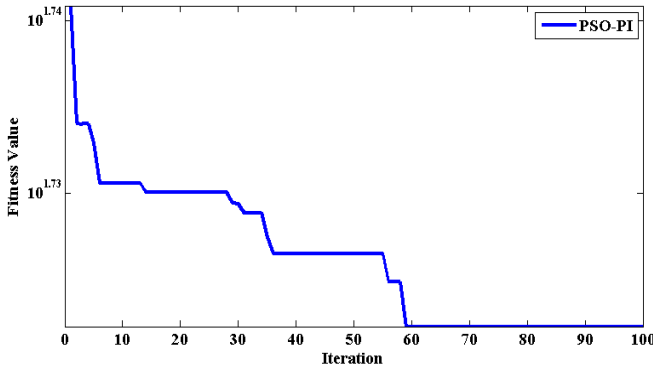


Fig.11b Best Fitness curve

#### 4.4 Gravitational Search Algorithm

GSA is a metaheuristic optimization method proposed by E.Rashedi et al in 2009 inspired from Newton's Gravitational law and mass interactions. The solutions in the GSA population are called agents. These agents interact with each other through gravity force and their performance is measured through its mass. Each agent is considered as an object and all objects move towards the other object with a heavier mass. This is considered as the global movement and the object with heavier mass moves slowly representing the exploitation step of the algorithm. The best solution is the solution with a heavier mass. This algorithm has a good ability to search for global optimum but its searching speed is slow during the last iterations. So a hybridization of PSOGSA is implemented to solve the problem.

#### 4.5 PSO-GSA

A new hybrid population- based algorithm. PSOGSA is the combination of Particle swarm optimization and Gravitational search algorithm. Two algorithms can be hybridized in low level or high level with relay or co-evolutionary method. The hybrid is low level since, the

functionality of both the algorithms are utilized and it is co-evolutionary since both the algorithms run in parallel. The main idea is to integrate the ability of exploration in GSA to synthesize both algorithm's strength.

#### 4.6 Implementation of Hybrid PSOGSA algorithm

The proposed hybrid PSOGSA optimization algorithm is implemented as follows. First, the PSO starts by generating the population. Initialise the particles by choosing random values for position and velocity. In each iteration the position and the velocity of the particles are calculated. Compute the gravitational constant  $G$  for all particles using the following equation.

$$\text{Gravitational constant } G(t) = G_0 \left( \frac{\alpha t}{T} \right) \quad (33)$$

Where  $\alpha$  and  $G_0$  descending Co-efficient and initial value respectively. According to the law of motion, the acceleration of an agent is proportional to the resultant force and inverse of its mass. So the acceleration of all the agents is given by

$$a_i^d(t) = F_i^d(t) / M_{ii}(t) \quad (34)$$

Where  $t$  is the specific time and  $M_i$  is the mass of the object  $i$ . In a problem space with the dimension  $d$ , the total force that acts on the agent  $i$  is calculated as

$$F_i^d(t) = \sum_{j \in K_{best}, j \neq i} rand_j F_{ij}^d(t). \quad (35)$$

Where  $rand_j$  is a random number in the interval  $[0,1]$ . During all epochs, the gravitational forces from agent  $j$  on agent  $i$  at a specific time  $t$  is defined as

$$F_{ij}^d(t) = G(t) M_{pi}(t) \times M_{aj}(t) \times (x_j^d(t) - x_i^d(t)) / R_{ij}(t) + \epsilon \quad (36)$$

Update the velocity and position of the agents at the next iteration using the equation.

$$v_i^d(t+1) = rand_i * v_i^d(t) + a_i^d(t) \quad (37)$$

$$x_i^d(t) = x_i^d(t) + v_i^d(t+1) \quad (38)$$

The process of updating the velocity and position ends when the stopping criterion is met.

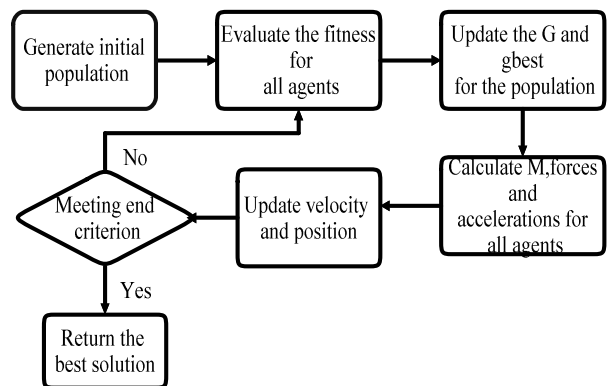


Fig.12. Flowchart for PSOGSA algorithm

Fig 12 shows the Flowchart for PSOGSA algorithm and the parameters for PSOGSA algorithm is tabulated in table 4.

**Table.4 Parameters of PSOGSA Algorithm**

Maximum iterations	100
Population size	100
Inertia weight w	1.0
Inertia weight damping ratio $w_{damp}$	0.99
Personal learning coefficient $C_1$	1.5
Global learning coefficient $C_2$	2.0
Lower bounds	0.01
Upper bounds	200
Number of variables	50

**Table.5 PSOGSA optimized Proportional gain and Integral gain values**

Controller	$K_p$	$K_i$	Best	Worst	Elapsed time
PSOGSA-PID	1.6266	2.5	29.5450	30.0046	65.3283

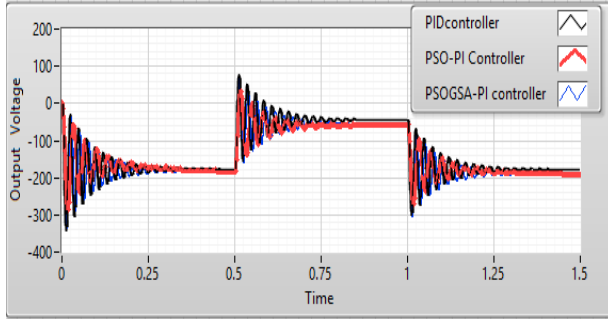


**Fig.13 Output voltage waveforms for optimized PSOGSA-PI controller**

Fig. 13 shows the output voltage waveform of the optimized PID controller. The graph was obtained by substituting the best  $K_p$  and  $K_i$  values obtained from optimization. The graph showing the best fitness value for each iteration was presented in Fig. 14.

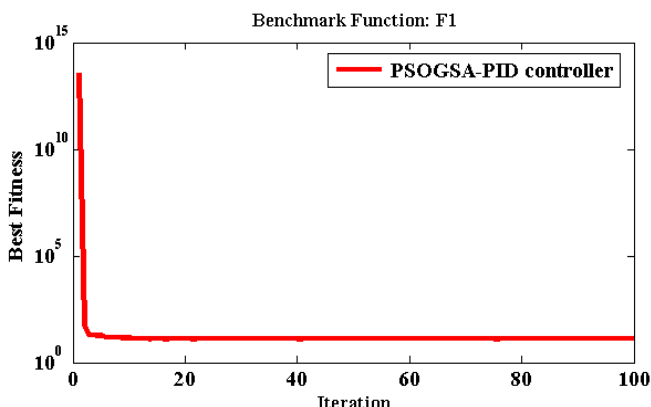


**Fig.14. Best fitness curve**

## 5. Conclusion

**Table.6 Performance indexes**

Controller	IAE	ISE	ITAE	ITSE
PI Controller	46.36	2908	69.54	4361
PSO-PI controller	40.68	2204	61.02	3306
PSOGSA-PID controller	37.75	2387	56.63	3581

Table 6 discusses the result on Performance indices of Cuk converter. From the table, it was observed that the IAE is reduced from 46.36 to 37.75 and ITAE is reduced from 69.54 to 56.63. Reduction in IAE and ITAE indicates that the Performance index with optimized PI controller was improved than with PI controller. With these results, it can be concluded that the PSOGSA optimized PI controller provides faster convergence and better solution in terms of Integral absolute error.

## References

1. Erickson, Robert W. Maksimovic, Dragan" Fundamentals of Power Electronics "Second edition by Springer US, 2001 website.
2. Graphical System Design Guide to Power Electronics Co-Simulation with Multisim and LabVIEW.
3. National Instruments Corp. Getting Started with Lab VIEW," April 2003 [Online].
4. H. C. Chiang, F. J. Lin, J. K. Chang, K. F. Chen, Y. L. Chen and K. C. Liu, "Control method for improving the response of single-phase continuous conduction mode boost power factor correction converter," in *IET Power Electronics*, vol. 9, no. 9, pp. 1792-1800, 7 27 2016.
5. P. Deivasundari, G. Uma and S. Ashita, "Chaotic dynamics of a zero average dynamics controlled DC-DC Cuk converter," in *IET Power Electronics*, vol. 7, no. 2, pp. 289-298, February 2014.
6. T.Mariamammal & T. Deepa,"Performance indices of Cuk converter implementing PI and PI-SMC controller", in *International Journal of Control Theory and Applications*, 9(2) 2016,pp 731-740.
7. Meryem Oudda, Abdeldjebar Hazzab," Photovoltaic system with SEPIC converter controlled by the fuzzy logic" in *International Journal of power electronics and drive systems*, vol 7, No 4, Dec 2016,pp 1283-1293.
8. Hossein Komijani, Saeed Masoumi Kazraji, Ehsan Baneshi, Milad Janghorban Lariche,"Modelling and state feedback controller design of tubular permanent magnet synchronous motor", in *International Journal of power electronics and drive systems*, vol 7, No 4,Dec 2016,pp 1410-1419.
9. R.K.Thakur, "Closed loop control analysis with feed-forward control of Cuk converter," 2014 Annual EE India Conference (INDICON), Pune, 2014, pp. 1-5.
10. Gunawan Dewantoro," Multiobjective optimization scheme for PID controlled DC motor", *International Journal of power electronics and drive systems*, vol 7, No 3, Sep 2016, pp 733-741.



11. Ola dimeji Ibrahim, Nor Zaihar B Yahaya, Nordin Saad," PID controller Response to set point change in DC-DC converter control", vol 7,No 2, June 2016, pp 294-302.
- 12.K. Trojanowski and T. Kulpa,"Particle convergence time in the PSO model with inertia weight," 2015 7th International Joint Conference on Computational Intelligence (IJCCI), Lisbon, Portugal, 2015, pp. 122-130.
- 13.N. Dey and T. Santra, "Application of PSO for optimizing gain parameters of a controller in real system," Michael Faraday IET International Summit 2015, Kolkata, 2015, pp. 30-35
- 14.Y. k. Wang and J. s. Wang, "Optimization of PID controller based on PSO-BFO algorithm," 2016 Chinese Control and Decision Conference (CCDC), Yinchuan, China, 2016, pp. 4633-4638.
- 15.E. Sahin, M. S. Ayas and I. H. Altas, "A PSO optimized fractional-order PID controller for a PV system with DC-DC boost converter," 2014 16th International Power Electronics and Motion Control Conference and Exposition, Antalya, 2014, pp. 477-481.
- 16.T.Deepa and P.Lakshmi,"Comparison of PI tuning using GSA and PSO for a Multivariable experimental four tank system", International Journal of Engineering and Technology, vol. 5 no. 6,Dec 2013-Jan 2014.